Available online at www.sciencedirect.com

ScienceDirect

Advances in Space Research 57 (2016) 527–542

ADVANCES IN SPACE RESEARCH (a COSPAR publication)

www.elsevier.com/locate/asr

Quantifying the tracking capability of space-based AIS systems

Andreas Nordmo Skauen

Norwegian Defence Research Establishment (FFI), P.O. Box 25, NO-2027 Kjeller, Norway

Received 2 July 2015; received in revised form 26 October 2015; accepted 23 November 2015
Available online 28 November 2015

Abstract

The Norwegian Defence Research Establishment (FFI) has operated three Automatic Identification System (AIS) receivers in space. Two are on dedicated nano-satellites, AISSat-1 and AISSat-2. The third, the NORAIS Receiver, was installed on the International Space Station. A general method for calculating the upper bound on the tracking capability of a space-based AIS system has been developed and the results from the algorithm applied to AISSat-1 and the NORAIS Receiver individually. In addition, a constellation of AISSat-1 and AISSat-2 is presented. The tracking capability is defined as the probability of re-detecting ships as they move around the globe and is explained to represent and upper bound on a space-based AIS system performance. AISSat-1 and AISSat-2 operates on the nominal AIS1 and AIS2 channels, while the NORAIS Receiver data used are from operations on the dedicated space AIS channels, AIS3 and AIS4. The improved tracking capability of operations on the space AIS channels is presented.

Keywords: AISSat-1; AISSat-2; NORAIS; AIS; Space-based AIS; Maritime surveillance

1. Introduction

The Norwegian Defence Research Establishment (FFI) has operated two Automatic Identification System (AIS) receivers in space since summer 2010. The first receiver put into operation was the NORAIS Receiver on-board the Columbus module of the International Space Station (ISS) in June 2010 (Eriksen et al., 2010). The AISSat-1 satellite was launched shortly thereafter in July (Narheim et al., 2011; Helleren et al., 2012a). In addition to demonstrating space based AIS as a maritime security and surveillance capability for European authorities, the receivers were designed to collect auxiliary data about the AIS signals and signal environment in space. The intention was to collect information that would contribute to the development of value added products (Skauen et al., 2013), more advanced decoding algorithms and investigate in-situ the challenges that space-based AIS receivers face (Skauen and Olsen, 2015).

Since the two receivers were put into operation in 2010 satellite AIS systems have gone from being an experimental service to being a fully operational capability. Authorities responsible for maritime safety and security worldwide are now more or less reliant on the capability that space-based AIS systems provide. The introduction of satellite AIS systems have provided an unprecedented ability to monitor ship traffic on a global scale (Eriksen et al., 2010) and the user feedback indicates that now that the light has been switched on, no one wants to go back into the dark. In order to maintain the satellite AIS service to Norwegian authorities a copy of AISSat-1, namely AISSat-2, was launched July 2014 to serve as an in-orbit spare for AISSat-1. Both satellites operate simultaneously, extending the maritime situational awareness that satellite based AIS systems provides.

This paper aims to quantify the tracking capability of the AISSat satellites and the improvement achieved by

E-mail address: Andreas-Nordmo.Skauen@ffi.no

http://dx.doi.org/10.1016/j.asr.2015.11.028
0273-1177/

adding AISSat-2 to the AISSat-1 service. Finally, the tracking capability of space-based AIS systems operating on the dedicated long-range AIS frequencies, AIS3 and AIS4, is investigated. While all three AIS receivers mentioned have the capability of operating on the AIS3 and AIS4 channels, only the NORAIS Receiver has performed long-term recordings on the long-range channels. AISSat-1 and AISSat-2 nominal operations are on the AIS1 and AIS2 channels. There are many other space-based AIS systems currently in operation in addition to the Norwegian assets, ranging from commercial companies such as ORBCOMM and exactEarth (Carson-Jackson, 2012; Posada et al., 2011), to institutional initiatives such as the German Aerospace Centre (DLR) AIsat satellite (Dembovskis, 2012) and the Japan Aerospace Exploration Agency (JAXA) SDS-4 satellite (Nakamura et al., 2013) to name a few from the many in each category.

The method used to quantify the tracking capability is general and can be implemented for any space-based AIS system to show the users of space-based AIS data what kind of tracking capability they can expect from a particular system. The only requirement is that the space-based AIS system affixes a timestamp to the AIS message upon reception. It is important to note that the tracking capability is not an AIS *receiver* performance measure (defined by a message detection probability by way of bit error rates vs. signal to noise ratios), but rather a space-based AIS *system* performance measure (defined by the capability of re-detecting ships as they move around the globe). The tracking capability, defined in Section 2, is a figure of merit for the users of space-based AIS systems (coast guards, coastal administrations, customs etc.) indicating the probability that the space-based AIS system can track ship movements around the globe and in their area of jurisdiction.

1.1. AISSat mission architecture

The overall AISSat (comprising AISSat-1 and AISSat-2) mission architecture and main ground site locations during FFI-led operations are shown in Fig. 1. The AISSat satellites receive AIS messages from ships at sea globally and forward the messages to the Svalbard ground station (78°N). In principle, the Svalbard location permits contact with an AISSat satellite in all of the satellites' 15 daily orbits. In practice, using only one antenna for downlink and uplink respectively, only one satellite can be contacted at a time in passes where both AISSat-1 and AISSat-2 are within contact range simultaneously. Since the satellites are in slightly different orbits, and neither satellite has on-board propulsion, the orbits will drift with respect to each other and will sometimes be over Svalbard simultaneously, sometimes half an orbit apart. There is roughly a 7 day period of increasing and decreasing overlap every 30 days.

The AIS messages are forwarded to the Norwegian Coastal Administration (NCA) in Haugesund, and finally to the Mission Control Centre (MCC) at FFI, Kjeller. Commands for tasking and operation of AISSat satellites are sent in the opposite direction. The NCA is responsible for distributing the AIS data to the users.

The satellites were built, tested and prepared for flight by the Space Flight Laboratory at the University of Toronto Institute for Aerospace Studies (UTIAS/SFL), and were based on the 20 cm cube Generic Nano-satellite Bus (GNB). UTIAS/SFL was also responsible for launch arrangements. AISSat-1 was launched by the Indian Polar Satellite Launch Vehicle (PSLV) from southern India July 2010, while AISSat-2 was launched with the Soyuz launch vehicle from Baikonur in Kazakhstan July 2014. Both launches were as secondary "piggyback" satellites. The payload, identical for the satellites, is an AIS receiver developed and manufactured by Kongsberg Seatex AS, Trondheim Norway. The AIS payload is a software defined radio that supports, and has been subject to, in-orbit upgrade of the payload algorithms, enabling higher performance. The Norwegian Defence Research Establishment (FFI), Kjeller, Norway developed the AISSat mission concept and has been responsible for managing the project, testing and preparing the AIS payload for flight, and analysing the data.

1.2. NORAIS Receiver mission architecture

The NORAIS Receiver was part of the Ship ID System on-board the ISS. The Ship ID System is a European Space Agency (ESA) project initiated mid-2008. A tight development schedule was imposed due to a window of opportunity for installing the system on board ISS, as well as mounting the VHF antenna on the outside of the Columbus module (European Space Agency, 2009). In order to comply with the schedule requirements, the NORAIS Receiver was based on the Kongsberg Seatex receiver developed for AISSat-1. The project has been led by FFI with support from ESA's General Support Technical Programme and is still on-going at the time of writing.

The NORAIS Receiver was commissioned 1st of June 2010 and was operated almost continuously until 1st of February 2015, when it was de-activated. The AIS data are downlinked via the ISS data network, forwarded to the Columbus Control Centre, then to the Norwegian User Operations Centre in Trondheim, Norway. FFI retrieve data files hourly with a latency of three hours. From the 51.6° inclination, 340–400 km altitude, orbit of the ISS the NORAIS Receiver does not have global coverage, rather from ~70° north to 70° south.

The NORAIS Receiver, like the AISSat receivers, is a software defined radio design operating across the maritime band from 156 to 163 MHz. The main reason for covering more than the two standard AIS frequencies (AIS1: 161.975 MHz, AIS2: 162.025 MHz) was to have the possibility to demonstrate the operational use of new channels in the maritime band to be allocated to space-based AIS (AIS3: 156.775 MHz, AIS4: 156.825 MHz). Also, this configuration allows characterization of the maritime VHF spectrum with respect to occupancy and interference. The

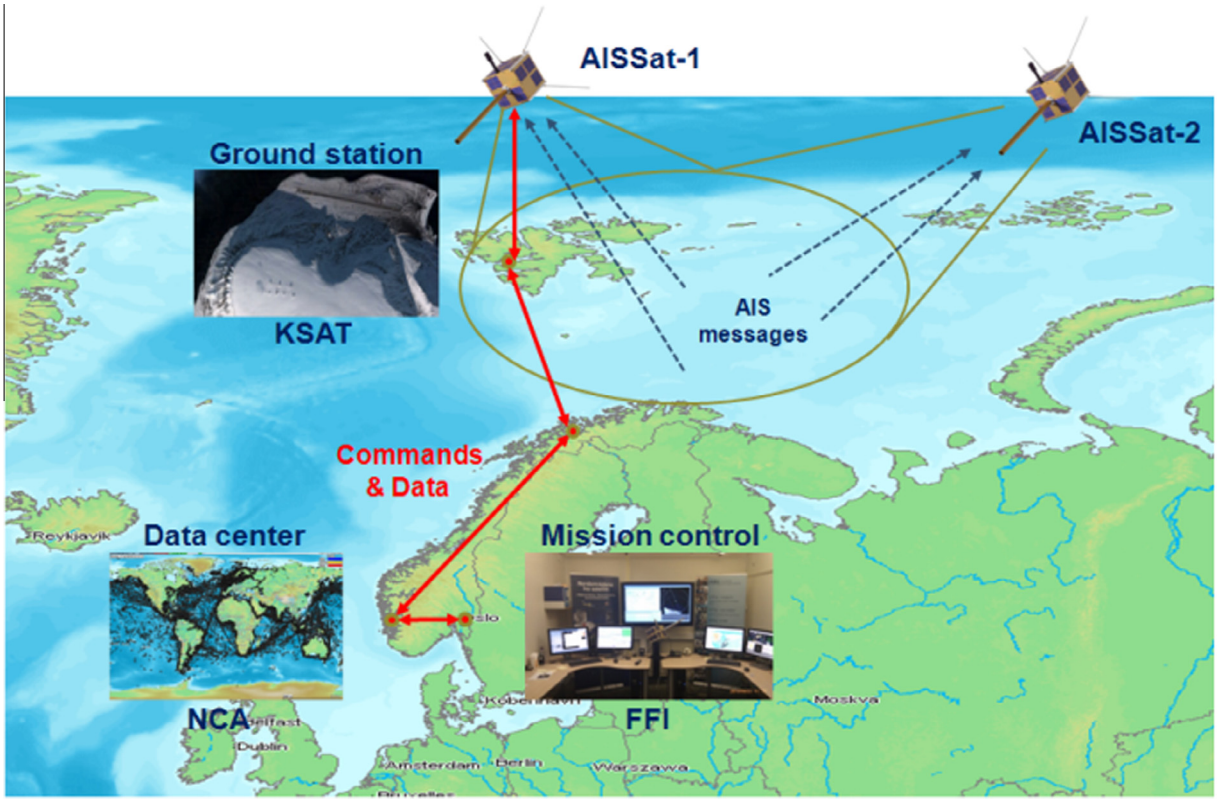

Fig. 1. AISSat-1 mission architecture.

software implementation allows for optimization of the receiver settings in orbit and also allows for upload of new signal processing algorithms. In May 2013 a final improved on-board algorithm was uploaded to the NORAIS Receiver with an on-average improved global performance of 25% with respect to number of messages and 20% with respect to number of unique MMSI detected. The improvements are greater in more difficult areas. The upgrade has also been implemented on the AISSat satellites and the results presented in this paper are all from the upgraded algorithm.

The NORAIS Receiver was replaced 1st of February 2015 by the next generation hardware named NORAIS-2. In addition to running even more advanced algorithms than the NORAIS Receiver, NORAIS-2 operates on all four AIS frequencies simultaneously, and can sample and store on-board up to 512 MByte of data while decoding on all four channels.

1.3. AIS system

The AIS system is fully described in the International Telecommunication Union recommendation ITU-R M.1371 (ITU, 2014). AIS is a ship-to-ship and ship-to-shore reporting system intended to increase the safety of life at sea and to improve control and monitoring of maritime traffic. AIS equipped ships broadcast their identity, position, speed, heading, cargo, destination, etc. to ships and shore stations within range of the VHF transmission. The nominal AIS channels are 161.975 MHz and 162.025 MHz, and the channels intended for long range use are 156.775 MHz and 156.825 MHz. The long range frequencies are referred to as the space AIS channels in this paper.

The message content and reporting intervals depend on the 27 types of messages, and dynamic conditions of the ship such as speed and rate of turn. The tracking method and re-detection probability calculations presented in this paper use only message types 1–3, transmitted on the nominal AIS channels, and type 27, transmitted on the space AIS channels. The message types 1–3 have dynamic content such as speed and position information and are transmitted every 2–10 s depending on the specific dynamic conditions, e.g. speed and rate of turn. If stationary or moving slower than 3 knots the reporting interval is 3 min. The long range type 27 message reporting interval is every 3 min regardless of dynamic conditions. The message type 27 content is reduced compared with the type 1–3 message types, but still contains position and speed information. All messages contain a unique identifier, the Maritime Mobile Service Identity (MMSI) number. The MMSI number may change if the ship changes owner or any other registration details, but is assumed to not change over the relatively short timescales investigated in this paper. Most AIS messages, including type 1–3 and 27, do not contain time information. However, knowing the time of reception is critical for virtually all applications utilizing AIS data. Depending on the space-based AIS system

ground station infrastructure, the AIS message downloaded can be several hours old and the reception time becomes important for integration with coastal AIS data. For the tracking method presented in this paper it is further critical that the clock providing the timestamp to the space-based AIS system is correct in order to verify that the positions transmitted in the AIS messages are within the field of view of the satellite. Finally, all AIS messages also contain a repeat flag indicator that is set if the message has been repeated by an AIS transponder other than the message originator. This repeat flag indicator is important for the purposes of tracking in this paper, again because of the timing difference between original and repeated messages.

In high density ship traffic areas, such as the Mediterranean, Gulf of Mexico, North Sea and East and South China Sea for example, co-channel interference will degrade the performance of a space-based AIS system drastically (Eriksen et al., 2006; Re et al., 2012). In addition there is evidence of strong land-based interference that also degrades the space-based AIS system performance when these interference sources are within the field of view (Skauen and Olsen, 2015). Co-channel and land-based interference effectively raises the average noise level, leaving some signals with negative or not a large enough signal to noise ratio for reliable reception for a specific AIS receiver. The significantly longer reporting interval of the type 27 message on the space AIS channels compared to the standard AIS reporting intervals should increase the space-based AIS system capacity markedly because the co-channel interference is reduced (ITU, 2009). However, the land-based interference will still cause significant problems when within the field of view of the space-based AIS system. Tracking capability results from operations on the space AIS channels are presented in Section 4 of this paper while results from operations on the nominal AIS channels are presented in Section 3. Section 2 presents the algorithm developed to obtain the tracking capability results, while Section 5 will discuss the results.

2. Methodology

A general method to estimate the tracking capability of space-based AIS sensors has been developed for the results presented in this paper. The results are based only on the data recorded by the space-based AIS sensors themselves. Ground truth data does not exist except close to land for coastal AIS network data, with stringent access restrictions limiting the area and ship type accessible for ship monitoring system (VMS) data (EU Commission, 2011) or with access restrictions depending on the ships' flag administration in the case of long-range identification and tracking (LRIT) data (Chen, 2014). Since no ground truth data is used, the tracking capability, or re-detection performance, results can be considered an upper bound on a space-based AIS system performance.

In order to quantify the tracking capability the following definitions are used:

- $N_{\text{det}}^{\text{MMSI}}(\text{grid cell})_{T_{\text{start}}}^{T_{\text{end}}}$: The number of space-based AIS system accesses to the grid cell in which an MMSI was detected within a specified timeframe between T_{start} and T_{end}.
- $N_{\text{tot}}^{\text{access}}(\text{grid cell})_{T_{\text{start}}}^{T_{\text{end}}}$: The total number of space-based AIS system accesses to the grid cell over the specified timeframe between T_{start} and T_{end}.

For detection, a single message is sufficient per access to the area. The total number of messages received per access is irrelevant for this tracking capability algorithm. As previously mentioned in the introduction, the tracking capability is not an AIS receiver performance measure, but rather a space-based AIS system performance measure.

The space-based AIS system tracking capability of a particular ship in a particular grid cell is quantified by Eq. (1).

$$TC_{\text{MMSI}}(\text{grid cell}) = \frac{N_{\text{det}}^{\text{MMSI}}(\text{grid cell})_{T_{\text{start}}}^{T_{\text{end}}}}{N_{\text{tot}}^{\text{access}}(\text{grid cell})_{T_{\text{start}}}^{T_{\text{end}}}}. \tag{1}$$

When a tracking capability for all grid cells for all MMSI used in the analysis has been quantified according to Eq. (1), a re-detection probability per grid cell is inferred from the average tracking capability per grid cell according to Eq. (2).

$$P_{\text{re-detection}}(\text{grid cell}) \sim TC(\text{grid cell}) = \frac{\sum_{\text{MMSI}} TC_{\text{MMSI}}(\text{grid cell})}{\text{Number of MMSI detected in the grid cell}} \tag{2}$$

In order to quantify the tracking capability as described by Eq. (1) and ultimately Eq. (2) the algorithm must, in general:

i. Calculate the space-based AIS system's access time to every grid cell per orbit over the specified timeframe from orbital mechanics in order to enable calculation of $N_{\text{tot}}(\text{grid cell})_{T_{\text{start}}}^{T_{\text{end}}}$.
ii. Remove MMSI identifiers used by more than one ship or reporting erroneous positions.
iii. Track the movements of each MMSI (ship) over the analysis timeframe in order to calculate $N_{\text{det}}^{\text{MMSI}}(\text{grid cell})_{T_{\text{start}}}^{T_{\text{end}}}$.
iv. Calculate the tracking capability per MMSI as per Eq. (1) and further quantify the average tracking capability for all MMSI per grid cell as per Eq. (2).

These steps are explained in further detail in subsequent sections.

2.1. Access time calculation

The first step of the algorithm is to calculate the series of the space-based AIS systems' access times to every grid cell on the globe over the analysis timeframe, denoted by $t(\text{grid cell})$. Typically a $2^\circ \times 2^\circ$ grid resolution has been used for a 15 day analysis timeframe. A lower bound on the analysis timeframe has not been investigated, but one must sensibly allow enough time for a large number of space-based AIS system accesses to each grid cell, and for the ships to move around in order for the tracking capability figure of merit to be representative of the space-based AIS system. For simplicity, two-line element sets from Space-Track have typically been used to propagate the orbit. If existing, the satellite systems recorded GPS or other navigation data could also be used of course. Of critical importance is that satellite clock is correct such that the time stamping of the AIS data is synchronised with the timestamp of the satellite navigation data. Otherwise, a problem may occur later in the algorithm because the space-based AIS system will have detected ships at a time when the space-based AIS system is reported by the navigation data to be elsewhere.

For convenience, in order to ensure that the algorithm only counts one access per grid cell per orbital period in the determination of $N_{\text{tot}}^{\text{access}}(\text{grid cell})_{T_{\text{start}}}^{T_{\text{end}}}$, only the first access time to each grid cell per orbit is stored and only intersection (partial coverage) with a grid cell is required for access. One could of course store all access times over the analysis timeframe, but one must somehow ensure that $N_{\text{tot}}^{\text{access}}(\text{grid cell})_{T_{\text{start}}}^{T_{\text{end}}}$ does not include multiple accesses per orbital period for a single satellite.

Since the algorithm aims to find the re-detection probability for a complete space-based AIS system, and not limited to individual satellites, a constellation access time is calculated if a constellation is investigated. For a constellation access time, the individual satellite access times are calculated and combined to a constellation access time in which multiple areas of the world are observed simultaneously. If no orbit maintenance is performed for the satellites in the constellation, the individual field of views may overlap from time to time, which is the case for AISSat-1 and AISSat-2 for instance. Such overlap must be reduced to a single access time such that the algorithm does not count two accesses to a grid cell for a single MMSI detection in that grid cell for instance, effectively halving the actual system re-detection probability for that MMSI in that grid cell. The algorithm defines overlap as multiple accesses to the same grid cell within 10 min, which is about the longest observation time of a grid cell possible for a satellite in 600 km altitude orbit. Other values may be used, depending on the figure of merit one is interested in. This is further explained in Section 2.3, detailing the tracking algorithm itself. When multiple access times to a single grid cell less than 10 min apart are found, the average access time is stored as the constellation access time for later use.

Because of potential refraction of the AIS signal in the ionosphere it is possible for the space-based AIS system to receive messages beyond line-of-sight. To account for beyond line-of-sight reception, the field of view from a satellite is typically increased by 20%, from trial and error investigating the data. The field of view itself will depend on the antenna configuration used by the space-based AIS system. The antenna patterns for AISSat-1, AISSat-2 and the NORAIS Receiver are approximated to be omnidirectional and the corresponding field of view extends to the horizon in all directions. In theory, a monopole antenna, as used by AISSat-1 and AISSat-2, has a null along the antenna axis. The dipole antenna used by the NORAIS Receiver has a similar null in addition to some shadowing by the ISS structure. These effects are assumed negligible for the access time calculations. The nulls are not large enough to cover an entire $2^\circ \times 2^\circ$ grid cell, and the extended field of view is used since in-orbit experience shows that the AIS messages are repeatedly received from beyond the horizon. Overall, it does not matter to an end user if a ship was not detected because the ship happened to be within the satellite antenna null, or whatever other reason, the end result is that the ship was not detected.

Accounting for beyond line-of-sight reception is important for the next step in the algorithm; removing re-used MMSI identifiers.

2.2. Removing re-used MMSI identifiers and MMSI identifiers reporting erroneous positions

In-orbit experience has shown that many MMSI identifiers are used by more than one ship. In order to calculate a tracking capability per MMSI, re-used MMSI must be removed. While it is often possible to separate multiple users with the same MMSI based on frequency shift information (Skauen et al., 2013), only about 0.5% of MMSI identifiers are removed because of suspected re-use. The impact on the re-detection probability is thus considered negligible.

In order to identify and remove re-used MMSI identifiers the algorithm calculates the speed required to move between the positions, in a straight great circle line, reported by each MMSI in the analysis timeframe, ordered by ascending time. When extracting the positions from the AIS messages received it is important to not include AIS messages that have the repeat flag set. If the repeat flag is set the AIS message is not transmitted by the reporting MMSI itself (ITU, 2014) and the timestamp, and subsequent speed calculation, will be wrong. If the calculated speed exceeds 60 knots and the distance travelled is greater than 300 m, the MMSI is excluded from further processing. The distance requirement is to allow for GPS inaccuracy, or hops, that sometimes occur, while excluding re-used MMSI identifiers within the same field of view.

Next, any MMSI identifiers reporting erroneous positions in the AIS messages are removed. Erroneous

positions are defined as positions outside the field of view, which is why the field of view was increased to allow for beyond line-of-sight reception. More refined techniques can also be used to verify if a reported position beyond line-of-sight is correct, or if an MMSI identifier is re-used within the same field of view, but the computation and complexity cost is high. If frequency shift information is available for instance, it is possible to verify if the reported positions have a frequency shift consistent with the expected frequency shift based on the geometry between the reported positions and the movement of the space-based AIS system. In order to calculate the expected frequency shift, the frequency bias of a particular ship transponder must be estimated from historic data and removed from the reported space-based AIS system reported frequency shift. Overall, less than 0.5% of MMSI identifiers are removed by reporting positions outside the (extended) field of view, after removal of re-used MMSI identifiers. Again, this effect is considered negligible on the overall result.

Messages reporting the default position 181°W, 91°N are not used by the algorithm such that no MMSI will be removed for having reported 181°W, 91°N during the analysis timeframe. The exception is if 181°W, 91°N is the only position the MMSI has reported during the analysis timeframe in which case it is difficult to track its movements. Again it could be possible to estimate the position based on frequency shift information (Skauen et al., 2013), but the computation cost and complexity is considered too much for the purposes of this algorithm. In the analysis timeframe considered in this paper, roughly 0.5% of the detected MMSI identifiers reported only 181°W, 91°N.

The remaining MMSI identifiers, not being re-used or reporting erroneous positions are then tracked over the analysis timeframe.

2.3. Tracking algorithm

The objective of the tracking algorithm is calculate the denominator of Eq. (1), $N_{\text{tot}}^{\text{access}}(\text{grid cell})_{T_{\text{start}}}^{T_{\text{end}}}$, i.e. the number of times, or passes, the space-based AIS system had access to a grid cell while a specific ship, or MMSI identifier, was present in the grid cell. The algorithm sensibly assumes that the ships may not be detected every time the space-based AIS system has access to the grid cell the ship has been detected, and must therefore estimate the start, $T_{\text{start}}(\text{grid cell})$, and end, $T_{\text{end}}(\text{grid cell})$, times based on a series of detections over time and analysis of the ship movements (i.e. tracking). Since a ship can move in and out of a grid cell many times during an analysis timeframe, it is important to sort the grid cells accessed by the MMSI identifier chronologically in order to get the sequence of grid cells visited correct.

In order to explain the analysis of ship movements around the grid the following nomenclature is used:

- Grid cell "n": The very first grid cell a ship is detected in during the analysis timeframe.
- Grid cell "k": The next grid cell after grid cell "n" a ship was detected in during the analysis timeframe.
- Grid cell "l": The next grid cell after grid cell "k" a ship was detected in during the analysis timeframe etc. Note that since the sequence of grid cells visited is ordered with respect to time, grid cell "l" can be the same grid cell as grid cell "n" if the ship made a U-turn for instance.
- $\tau_{\text{min / max}}(\text{grid cell})$: Timestamp of the ship reported position in the AIS message, affixed by the space-based AIS sensor upon reception.
- $t(\text{grid cell})$: The complete series of space-based AIS system access times to the grid cell during the analysis timeframe. Since only one access time is saved per orbital period per satellite, the access time is also referred to as a pass as per Section 2.1.
- $T_{\text{start/end}}(\text{grid cell})$: The start and end time estimated that the ship was present in the grid cell, expanded by an adjustment factor, δ.
- δ: Timestamp adjustment constant to ensure that the space-based AIS system access times, $t(\text{grid cell})$, used in the calculations are enveloped by the start and end times, $T_{\text{start/end}}(\text{grid cell})$, such that all relevant accesses when a ship was estimated to have been present in the grid cell are counted.

For a single satellite the timestamp adjustment constant, δ, can be set to half an orbital period, ca. 45 min for a 600 km altitude satellite. This will envelop the estimated timeframe a ship was present in a grid cell, without including previous or future space-based AIS system access times to the grid cell. For a constellation the constant will in effect be the minimum time between repeated ship detections by the constellation that should be counted as separate detections. For a constellation the constant should as such be set to a meaningful number for end-users to benefit from the separate detection performance. It does not add to the end-user utility if a ship is detected by another satellite in a constellation within a minute of the previous detection. If the detections are 10 min apart however, as used in the results presented in this paper, information about the ship movement may be gleaned. If the value is set higher, e.g. 30 min, the result will be the re-detection probability after a minimum of 30 min, even though the space-based AIS system could re-detect after only 10 min for example.

For the very first grid cell "n" each MMSI identifier has been detected in, the start time, $T_{\text{start}}(n)$, is set to the first space-based AIS system access time to the grid cell "n" according to Eq. (3). This selection is made in order to include any space-based AIS system accesses to the grid cell "n" in the analysis timeframe before the MMSI was detected the first time. The algorithm thus assumes that all MMSI detected have always been present, but were not necessarily always detected.

$$T_{\text{start}}(n) = \min t(n). \tag{3}$$

The end time for that same grid cell, $T_{\text{end}}(n)$ however, depends on the ship movements.

The simplest case is when the ship has moved from grid cell "n" into a new, neighbouring, grid cell "k" outside of a pass. More complex cases occur when a ship has moved out of grid cell "n" and into grid cell "k" during a pass, or even moved between the two grid cells multiple times during a pass. The latter can occur for example if a ship is moving precisely on, and parallel, to the grid boundary lines and the ship movements or inaccuracies in the reported position causes one message position to be on one side of the boundary line and another to be on the other side of the boundary line. Finally, if detection in the new grid cell "k" occurred long after, and far away from, detection in the previous grid cell "n", one has no way of knowing which other grid cells the ship has visited in the meantime. For the latter case, the algorithm used for the results presented in this paper splits the number of accesses between detections evenly between the two grid cells "n" and "k". The method for splitting the number of accesses evenly is described later.

In general, if the condition of Eq. (4) is satisfied, exemplified with the use of grid cells "n" and "k", the ship has moved between grid cells during a pass. If the condition is not satisfied, the move between the grid cells occurred while the space-based AIS system did not have access to the grid cells, i.e. outside of a pass (or the space-based AIS system did not detect the ship during the pass when the movement occurred and is similarly classified as movement outside of a pass, for which the rationale is discussed later.)

$$\tau_{\min}(k) - \tau_{\max}(n) \leqslant \delta \tag{4}$$

The two conditions and the three outcomes for the end time of grid cell "n", $T_{\text{end}}(n)$, are presented in Eq. (5).

If the condition of Eq. (4) is not satisfied however, the outcomes of Eq. (5), are more complicated since the ship has moved between grid cells when the space-based AIS system either did not detect the ship, or did not have access to the grid cells. Since one knows a posteriori the time between the last and first detections in grid cells "n" and "k" respectively, from $\tau_{\max}(n)$ and $\tau_{\min}(k)$, one also knows the number of accesses to grid cell "k", $N_{\text{tot}}^{\text{access}}(k)_{\tau_{\max}(n)+\delta}^{\tau_{\min}(k)-\delta}$, during the time between detections. One also knows the number of accesses to grid cell "n" of course, but the described algorithm makes a selection based on the number of accesses to grid cell "k" only. Since the selection is done only for the timeframe between detections in grid cells "n" and "k", it is impossible to know which grid cell the ship was actually in, but a decision must be made and in this algorithm the number of accesses to grid cell "k" is used for selection.

Because of the uncertainty regarding which grid cell the ship was in while not detected, if there is only one access to grid cell "k" between detections (outcome two of Eq. (5)), the algorithm assumes the ship was in the original grid cell "n" during the access without detection. Outcome two of Eq. (5) then specifies in words that the end time for grid cell "n", $T_{\text{end}}(n)$, is set to the last space-based AIS system access time to the grid cell "n", $t(n)$, **prior** to the time of the first message received in the next grid cell "k" from the MMSI tracked, $\tau_{\min}(k)$. Subtracting the adjustment factor, δ, from $\tau_{\min}(k)$ ensures that one does not estimate that the ship was in grid cell "n" during the same pass the ship was detected in grid cell "k".

If the number of accesses to grid cell "k" between detections is two or more however, the bottom outcome of Eq. (5) specifies in words that the end time for grid cell "n", $T_{\text{end}}(n)$, is set to the middle access time to grid cell "n", middle $t(n)$, between the last detection of the ship in grid cell "n", $\tau_{\max}(n)$, and the first detection in grid cell "k", $\tau_{\min}(k)$. If

$$T_{\text{end}}(n) = \begin{cases} \tau_{\max}(n) + \delta & , \tau_{\min}(k) - \tau_{\max}(n) \leqslant \delta \\ \max t(n) < \tau_{\min}(k) - \delta, & \tau_{\min}(k) - \tau_{\max}(n) > \delta,\ N_{\text{tot}}^{\text{access}}(k)_{\tau_{\max}(n)+\delta}^{\tau_{\min}(k)-\delta} \leqslant 1 \\ \tau_{\max}(n) + \delta < \text{middle}\, t(n) < \tau_{\min}(k) - \delta & , \tau_{\min}(k) - \tau_{\max}(n) > \delta,\ N_{\text{tot}}^{\text{access}}(k)_{\tau_{\max}(n)+\delta}^{\tau_{\min}(k)-\delta} > 1 \end{cases}. \tag{5}$$

If the condition of Eq. (4) is satisfied, i.e. the ship has moved between grid cells during a pass, the outcome of Eq. (5) (top) specifies in words that the end time of grid cell "n", $T_{\text{end}}(n)$, is set to the time of the last message received in the grid cell during the pass, $\tau_{\max}(n)$, plus the adjustment factor, δ. This ensures that $T_{\text{end}}(n)$ envelopes all relevant space-based AIS system access times in the grid cell "n", $t(n)$.

the number of accesses is an uneven number, the middle access time in effect attributes the greatest number of no detection passes to the original grid cell "n", similar to outcome two of Eq. (5). If the number of accesses between detections is even however, the middle access time is set to the maximum access time in the lower half of the access times in between detections, in effect evenly distributing the accesses without detection between grid cells "n" and "k".

All outcomes are adjusted by a factor, δ, to ensure that all relevant space-based AIS system access times, with only the first access time to a grid cell per pass saved as described in Section 2.1, are enveloped within the start and end times the ship is estimated to have been present in a grid cell, $T_{\text{start/end}}(\text{grid cell})$.

The start time, $T_{\text{start}}(k)$, of grid cell "k" is determined in a similar manner by evaluating the condition of Eq. (4), resulting in the two conditions of Eq. (6).

$$T_{\text{start}}(k) = \begin{cases} \min t(k) \geqslant T_{\text{end}}(n) + \delta, & \tau_{\min}(k) - \tau_{\max}(n) > \delta \\ \tau_{\min}(k) - \delta, & \tau_{\min}(k) - \tau_{\max}(n) \leqslant \delta. \end{cases} \tag{6}$$

In words, the first condition of Eq. (6), in the case where the movement from grid cell "n" to grid cell "k" occurred outside of a pass, specifies that the start time of grid cell "k", $T_{\text{start}}(k)$, is set to the first space-based AIS system access time to the grid cell "k" **after** the end time used for the previous grid cell "n", $T_{\text{end}}(n)$, plus the adjustment factor, δ, to ensure that $T_{\text{start}}(k)$ does not envelope the space-based AIS system access time, max $t(n)$, used in calculating the number of accesses in the previous grid cell "n".

If the condition of Eq. (4) is satisfied however, the outcome of Eq. (6) (bottom) specifies in words that the start time of grid cell "k", $T_{\text{start}}(k)$, is set to the time of the first message received in the grid cell, $\tau_{\min}(k)$, less the adjustment factor, δ, to ensure that $T_{\text{start}}(k)$ envelops all relevant space-based AIS system access times to grid cell "k", $t(k)$.

An illustration of tracking and estimation of the start and end times for several grid cells, $T_{\text{start/end}}(\text{grid cell})$, is shown in Fig. 2. Only movement between grid cells outside of a pass, with no accesses without detection, is illustrated.

The end time for presence in grid cell "k", $T_{\text{end}}(k)$, and the start time for presence in the next grid cell "l", $T_{\text{start}}(l)$, and so on are estimated in the manner described above by Eqs. (5) and (6) respectively, constantly checking the condition of Eq. (4) to determine grid cell crossings during or out of pass.

For the final grid cell, "z" a ship is detected in, the end time, $T_{\text{end}}(z)$, is set to the last space-based AIS system access time to the grid cell "z" in the analysis timeframe, according to Eq. (7)

$$T_{\text{end}}(z) = \max t(z). \tag{7}$$

Once $T_{\text{start}}(\text{grid cell})$, and $T_{\text{end}}(\text{grid cell})$ has been estimated for a grid cell, $N_{\text{tot}}^{\text{access}}(\text{grid cell})_{T_{\text{start}}}^{T_{\text{end}}}$ of Eq. (1) is easily counted as the number of space-based AIS system access times to the grid cell within the estimated timeframe.

The numerator of Eq. (1), $N_{\text{det}}^{\text{MMSI}}(\text{grid cell})_{T_{\text{start}}}^{T_{\text{end}}}$, which is the number of detections is counted directly from the number of AIS messages from the MMSI identifier in the grid cell. In order to only count one detection per space-based AIS system access time, the counting requires that the AIS messages are separated in time by an amount greater than the adjustment factor, δ.

2.4. Quantifying the tracking capability

When both $N_{\text{det}}^{\text{MMSI}}(\text{grid cell})_{T_{\text{start}}}^{T_{\text{end}}}$ and $N_{\text{tot}}^{\text{access}}(\text{grid cell})_{T_{\text{start}}}^{T_{\text{end}}}$ of Eq. (1) have been calculated for all the MMSI detected in the analysis period, following the steps in Sections 2.1–2.3, the tracking capability per MMSI per grid cell can

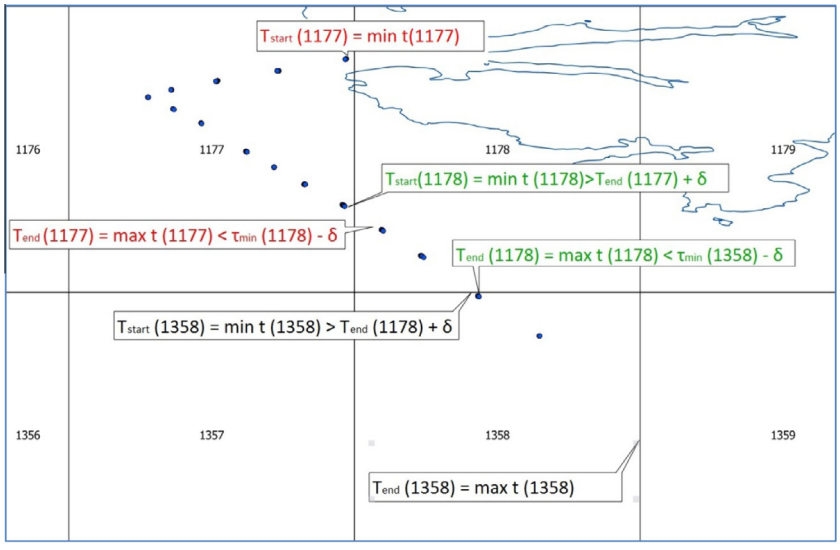

Fig. 2. Illustration explaining how the timeframe in which a ship was present in a grid cell is estimated. For example, the algorithm estimates that the timeframe the ship was present in the first grid cell the ship was detected in, 1177, is from the start of the analysis period, i.e. the first access time calculated (top red), until the last access time to grid cell 1177 prior to the first detection time in grid 1178 (bottom red). Similarly, the start and end times for grid cell 1178 are illustrated in green, and in black for very last grid cell, 1358, the ship was detected in. T, t, τ and δ are defined in Section 2.3. In this example, there were no accesses without detection and the track covers the entire analysis period.

be quantified according to Eq. (1). The final re-detection probability per grid cell, for any MMSI, is then inferred from the average tracking capability per grid cell according to Eq. (2).

This re-detection probability will represent an upper bound on the space-based AIS system re-detection probability for several reasons. Most importantly, MMSI identifiers that are never detected, and should contribute negatively to the re-detection probability, are naturally not included. The effect is greatest in the high traffic zone regions close to and including the North Sea, English Channel, Baltic Sea, Mediterranean Sea, Black Sea, East and South China Sea, Sea of Japan and the Gulf of Mexico. In these areas there is significant co-channel and land-based interference as described in Section 1.3. As a result of the interference challenge a great number of MMSI identifiers are never detected in these areas. Extending the analysis timeframe could help since the probability of receiving at least one message from a previously undetected MMSI identifier increases with increasing total observation time, but the re-detection probability will always be exaggerated in these areas.

There is also a time-edge effect introduced since the algorithm cannot know if an MMSI identifier has always been present, which is reasonable, and always transmitting AIS messages, which is more uncertain. The algorithm assumes that all MMSI identifiers have always been present, and every MMSI is assumed to have been in the first grid cell it was detected in for the entire timeframe from the start of the analysis period until the first detection time. Likewise, the algorithm assumes that every MMSI identifier is present in the final detection grid until the end of the analysis timeframe. This is a conservative approach, since ships may change MMSI numbers or stop transmitting during the analysis period.

Once the average re-detection probability per grid cell has been calculated from Eq. (2), the results can be statistically accumulated to show the temporal evolution of the re-detection probability as the space-based AIS system observes a grid cell multiple times according to Eq. (8).

$$P^{\text{accumulated}}_{\text{re-detection}}(\text{grid cell}) = 1 - \prod_{1}^{N^{\text{accumulated}}_{\text{accesses}}(\text{grid cell})} (1 - P_{\text{re-detection}}(\text{grid cell})). \quad (8)$$

where $N^{\text{accumulated}}_{\text{accesses}}$ is the number of space-based AIS system accesses to a grid cell within the accumulation time, calculated from orbital mechanics as per Section 2.1.

Typically the re-detection probability after 12 and 24 h have been presented. It is important to remember that the space-based AIS system orbit configuration and start location for the 12/24 h accumulation will determine the number of passes with access to a particular grid cell, and by extension influence the re-detection probability map. As such the resulting map is unique for that particular space-based AIS system. Simply put, a space-based AIS system with a single polar orbiting satellite will produce a very different map compared with a system of ten satellites in an equatorial orbit even if both systems use the same AIS receiver in the satellite(s).

The re-detection probability is generally overestimated when statistically accumulating. Statistical accumulation assumes there is an equal chance of detecting all ships, but in reality some ships are harder to detect because of poor AIS equipment installation or configuration, or the ships are at rest, transmitting few AIS signals for the space-based AIS system to receive. Investigations of individual ships have shown that messages from some ships always have high received signal strengths, whereas messages from other ships always have low received signal strengths. By extension, there will be some ships that always have transmitted signal strengths too low to be received by the space-based AIS system. The high traffic zones are particularly impacted. Comparison with coastal AIS data has shown that the presented re-detection probabilities fit best for moving ships (that are by nature transmitting more AIS messages, making them easier to detect) (Helleren et al., 2012b).

With these assumptions and caveats in mind, the resulting re-detection probability maps can be summarised as the upper bound re-detection probability for moving ships in the high seas.

3. Ship tracking capability on AIS1 & AIS2

The ship tracking capability on the nominal AIS channels is presented for the single AISSat-1 satellite and the combination of AISSat-1 and AISSat-2 in Sections 3.1 and 3.2 respectively. The results are based on data gathered over the 15 days between 25th August 2014 and 9th September 2014 for both satellites and the method presented in Section 2.

3.1. AISSAT-1

The tracking capability of AISSat-1 is presented in Fig. 3. In total 52,222 MMSI identifiers were tracked after removing 549 MMSI identifiers from the dataset because of MMSI re-use or reporting a position outside the satellite field of view. The results present the probability of re-detecting an already detected MMSI identifier in the first possible opportunity after an original detection.

The results show, unsurprisingly, that in areas with low ship traffic density, such as the Pacific Ocean and extreme northern latitudes the tracking capability, and re-detection probability, is high. Likewise, in areas with a high ship density, and thus co-channel interference issues when viewed from space, such as the Gulf of Mexico, Mediterranean, English Channel, North Sea, Baltic Sea, South and East China Sea, the re-detection probability is low. Signal environment mapping of the AIS channels from space have also indicated that there are sources of interference on land that are often within the field of view of a

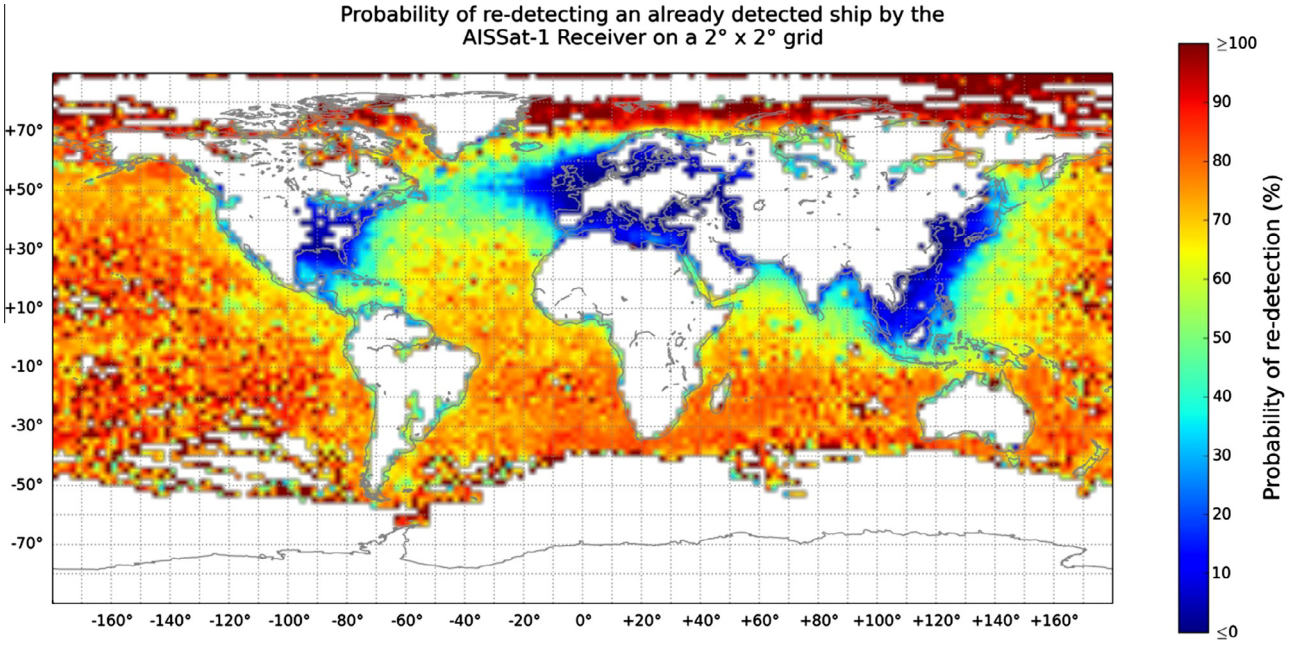

Fig. 3. First access time probability of re-detecting an already detected ship using the AIS1 and AIS2 channels by AISSat-1.

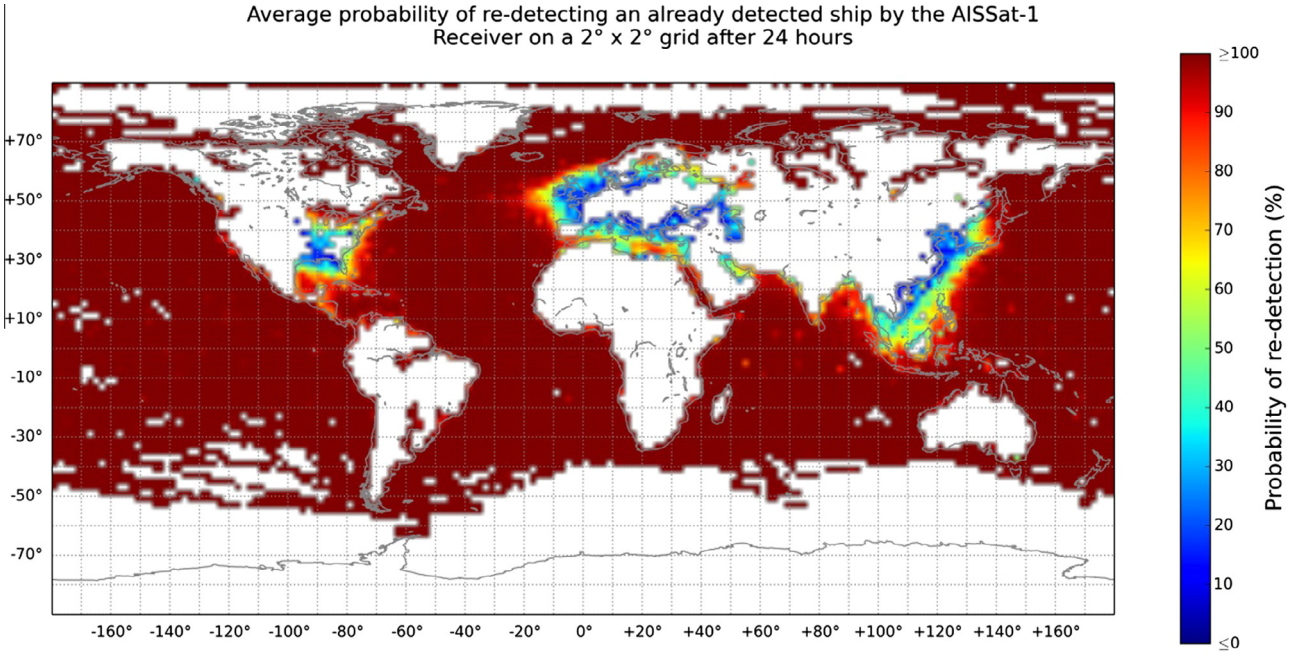

Fig. 4. Statistically accumulated probability of re-detecting an already detected ship using the AIS1 and AIS2 channels by AISSat-1 within 24 h.

space-based AIS system at the same time as the high traffic zones, degrading the system performance further (Skauen and Olsen, 2015). In the primary area of interest of the AISSat programme, the Norwegian High North, the performance is excellent. The AISSat-2 satellite is for all intents and purposes identical, and the result of Fig. 3 is representative for AISSat-2 as well.

Statistically accumulating the results in Fig. 3 over 24 h, taking into account the AISSat-1 orbit, yields the results in Fig. 4. The result presented in Fig. 4 fully establishes the utility of space-based AIS as a global maritime surveillance capacity. However, when viewing the result it is important to remember the caveats of statistical accumulation and of the method used. The performance is generally overestimated, but most significantly in the high ship density areas. For moving ships in the high seas the results are considered representative.

3.2. AISSAT-1 & AISSAT-2 combined

The tracking capability of AISSat-1 and AISSat-2 combined is presented in Fig. 5. In total 55,787 MMSI

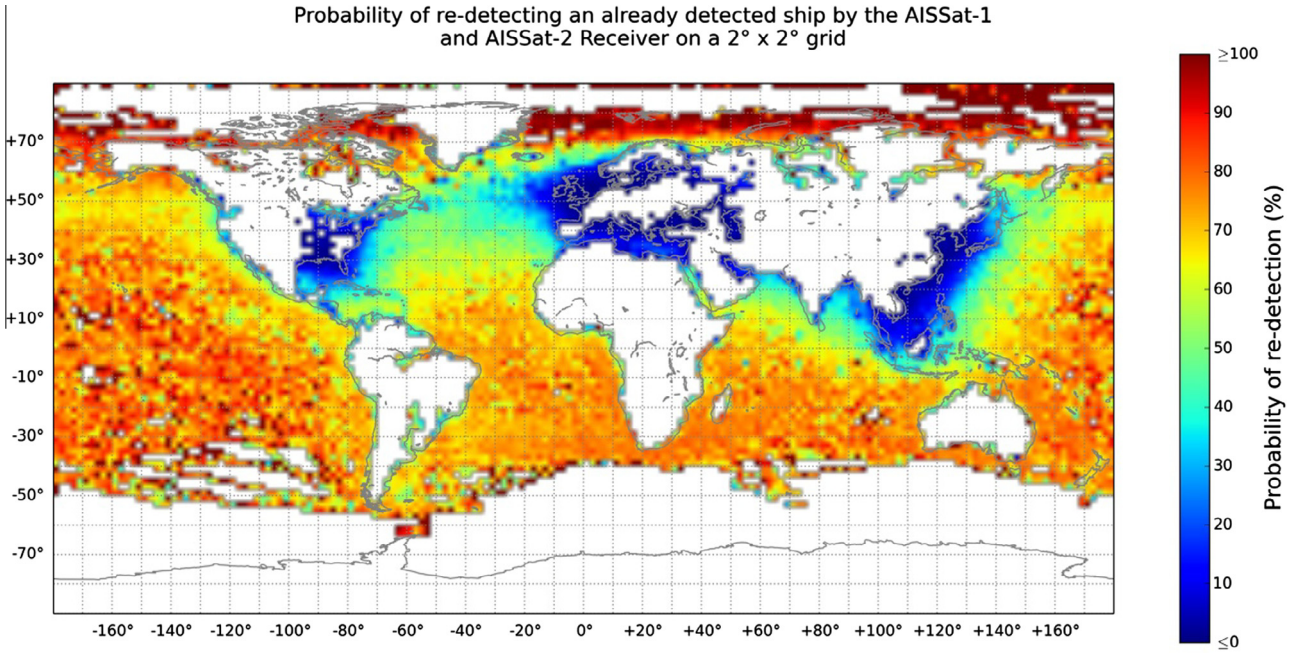

Fig. 5. First access time probability of re-detecting an already detected ship using the AIS1 and AIS2 channels by AISSat-1 and AISSat-2 constellation.

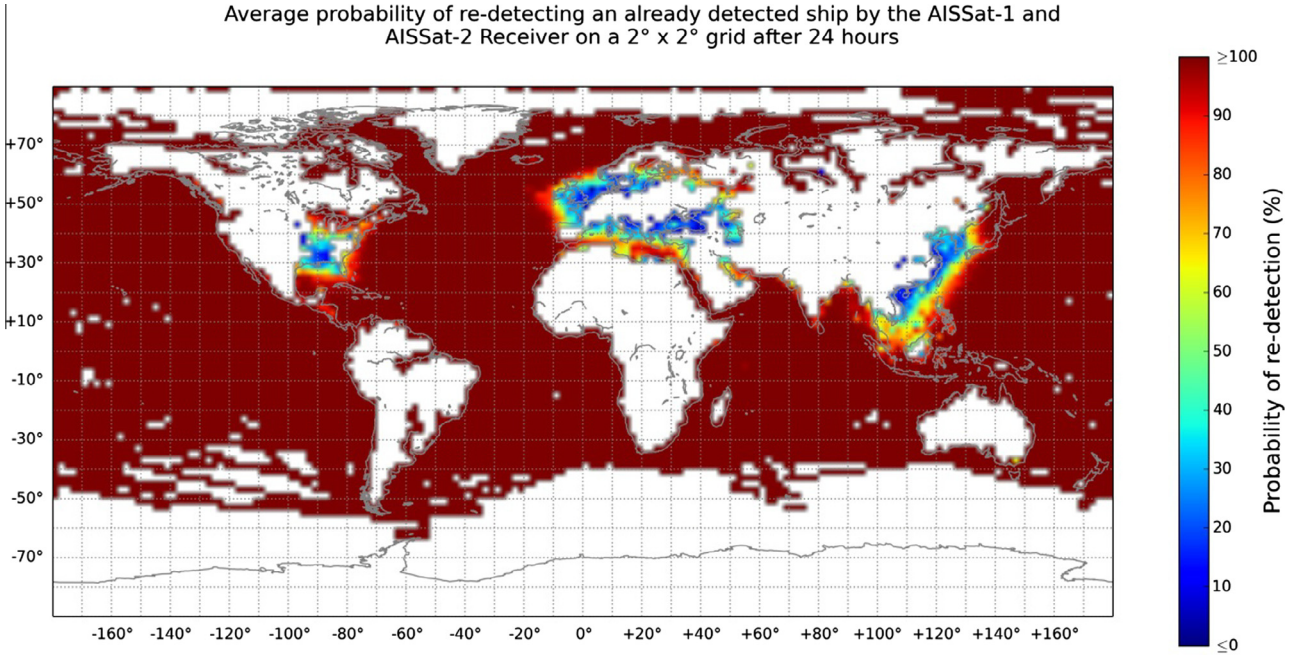

Fig. 6. Statistically accumulated average probability of re-detecting an already detected ship using the AIS1 and AIS2 channels by AISSat-1 and AISSat-2 constellation within 24 h.

identifiers were tracked after removing 549 of 52,222 MMSI identifiers from the AISSat-1 dataset and 355 of 52,017 from the AISSat-2 dataset because of MMSI re-use or reporting a position outside the satellite field of view. 303 of the removed MMSI identifiers were found in both AISSat-1 and AISSat-2 datasets.

Statistically accumulating the results in Fig. 5 over 24 h, taking into account both AISSat-1 and AISSat-2 orbits, yields the results in Fig. 6. As mentioned previously in Section 1.1, AISSat-1 and AISSat-2 are in slightly different orbits, and neither satellite has on-board propulsion. As such the orbits will drift with respect to each other and will sometimes cover the same area simultaneously, sometimes half an orbit apart. There is roughly a 7 day period of increasing and decreasing overlap every 30 days. The 15 day period analysed in this paper represents an average

coverage, with some overlap and some period where the satellites are maximally apart. The average 24 h coverage within the 15 day period is used to represent the 24 h re-detection probability. For a specific 24 h period, the actual orbit configuration of the two satellites for the specific 24 h period may yield a different result, but on average the results presented are what can be expected.

Compared with the re-detection probability of AISSat-1 alone, shown previously in Fig. 4, it is apparent that the areas of low re-detection probability shrink in size and the performance in the North Atlantic Ocean approaches the >95% re-detection probability of other open ocean areas.

An alternative benefit of a constellation is that one can achieve a similar re-detection probability as an individual satellite in the constellation in a much shorter timeframe. Statistically accumulating an average 12 h period for the AISSat-1 and AISSat-2 constellation yields the result of Fig. 7, which is very similar to that achieved by the single AISSat-1 satellite over a 24 h period in Fig. 4. Again it must be emphasised that for a specific 12 h period the specific orbit configuration of the constellation must be used, and that Fig. 7 represents the average 12 h re-detection probability expected.

4. Ship tracking capability on AIS3 & AIS4

The ship tracking capability on the space AIS channels is presented for the NORAIS Receiver in Section 4.1. The results are based on data gathered over the 31 days between 20th March 2014 and 20th April 2014 and the method presented in Section 2.

The AIS3 and AIS4 channels are allocated for transmission of message type 27, designed for reception in space. The longer reporting interval of the type 27 message reduces the likelihood of message collision at the space-based AIS receiver, thereby increasing the space-based AIS system capacity (ITU, 2009). However, with a longer reporting interval the space-based AIS receiver has fewer opportunities to receive the type 27 AIS message, and the performance of the AIS receiver is increasingly important in reliably receiving type 27 messages. As previously mentioned in Section 1.3, signal environment mapping unfortunately indicates that there is land-based interference on the AIS3 and AIS4 channels that will be in view of a space-based AIS system precisely at the same time as the high traffic zones areas, where the space-based AIS system performance gain would be the greatest using the new channels.

While the AISSat satellites can also operate on the space AIS channels, the AIS receiver can only operate on two channels simultaneously. Since the AISSat satellites are delivering an operational capability, and few ships are using the space AIS channels, the AISSat satellites have for all intents and purposes only operated on the nominal AIS channels. The NORAIS Receiver does not deliver an operational capability and is fully allocated to experimentation.

4.1. NORAIS Receiver

The tracking capability of the NORAIS Receiver, operating on the space AIS channels, is presented in Fig. 8. In total 2255 MMSI identifiers were tracked after removing 6

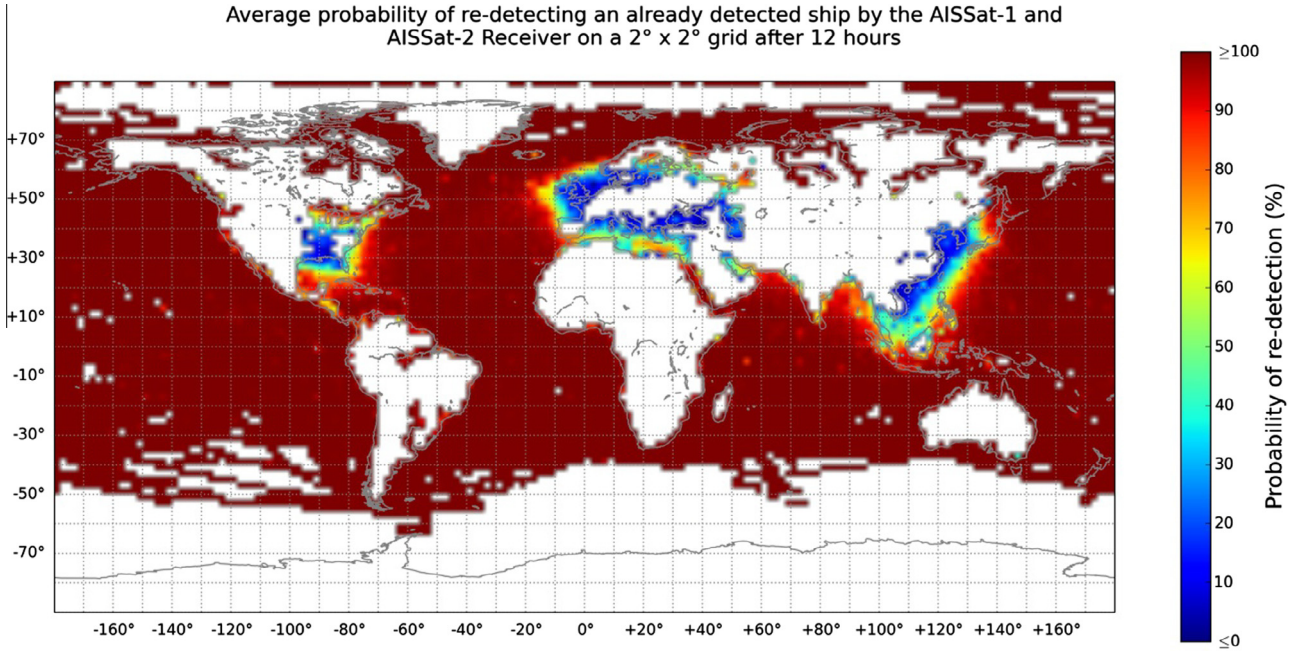

Fig. 7. Statistically accumulated average probability of re-detecting an already detected ship using the AIS1 and AIS2 channels by AISSat-1 and AISSat-2 constellation within 12 h.

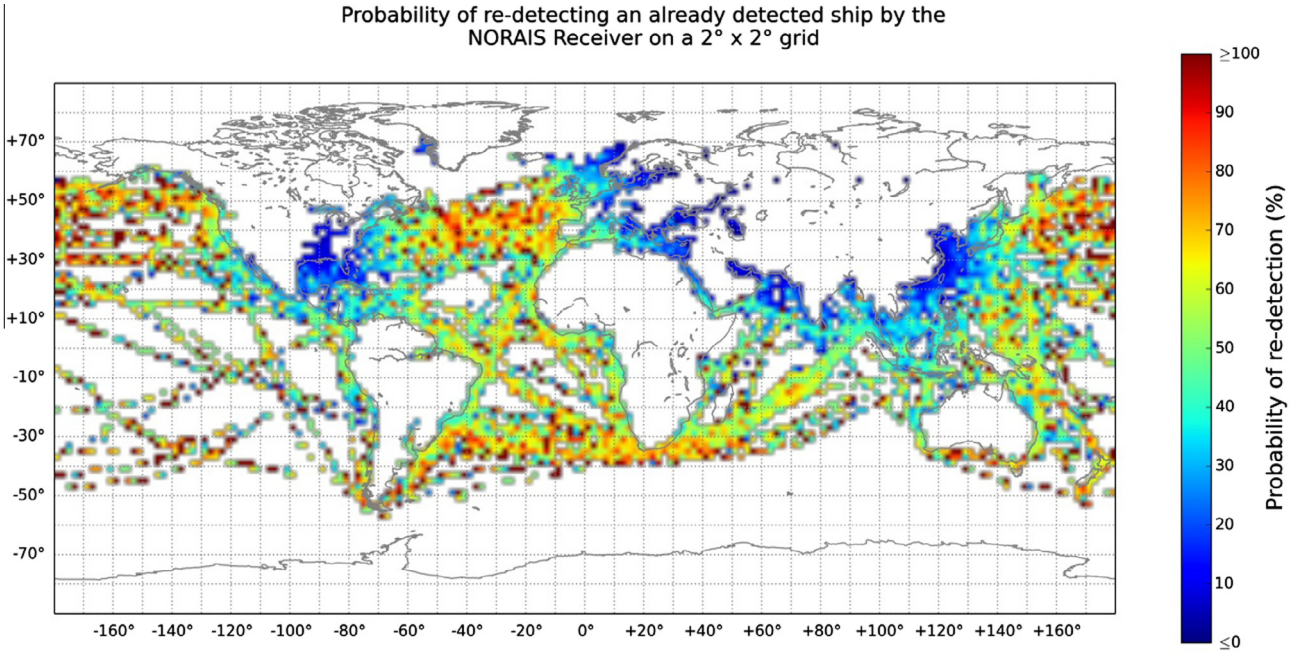

Fig. 8. First access time probability of re-detecting an already detected ship using the AIS3 and AIS4 channels by the NORAIS Receiver.

MMSI identifiers from the dataset because of MMSI re-use or reporting a position outside the satellite field of view.

Comparison with previously presented results from the AISSat satellites is not straightforward. While the AIS receiver hardware is mostly identical, and the same decoding algorithms are used, the ISS and the AISSat platforms are very different in terms of the local interference created. The noise floor of the NORAIS Receiver system is significantly higher than for the AISSat satellites, which is not surprising given the amount of equipment installed on the ISS. In addition, the orbits are very different. As well as not covering the extreme northern and southern latitudes, the lower ISS orbit can sometimes benefit from a smaller field of view. In particular in the North Atlantic Ocean, the AISSat satellites nearly always have a high density ship traffic area within the field of at the same time, while the NORAIS Receiver does not. Finally, the number of users is much lower such that in some areas, such as to the south of New Zealand and Australia and in the southern Pacific Ocean for instance, the statistics of the space AIS channel performance is not reliable.

Despite this higher system noise floor, the tracking capability on the space AIS channels show signs of noticeable improvement compared with the tracking capability on the nominal AIS channels. The re-detection probability is higher further into the high ship density areas of the English Channel, North Sea and Mediterranean, although these areas are still problematic because of the land-based interference previously discussed. The performance in the North Atlantic Ocean is also significantly higher, but this is to some extent also affected by the different orbits.

Statistically accumulating the results in Fig. 8 over 24 h, taking into account the ISS orbit, yields the results in Fig. 9. After 24 h the improved performance in the high density traffic areas is plain compared with even the combined effort of both AISSat-1 and AISSat-2 on the nominal AIS channels presented in Fig. 6. Operating on the space AIS channels it is possible to track and follow ships on a daily basis even in the high ship density areas using a space-based AIS system.

5. Discussion

Confidence in the results of the presented method can be achieved by comparison with other reference data sets, such as coastal AIS, VMS and LRIT data, mentioned in Section 2. In contrast to the openly broadcasted messages of the AIS system, VMS and LRIT are closed systems where only authorised users have access to the data. Examples of authorised users are governmental departments in charge of fisheries control, coastal administration, coast guard, police and customs. FFI has made comparisons between a space-based AIS system operating on the nominal AIS channels with all these sources and found acceptable agreement with the results from the method presented. Because of the aforementioned data policy, only comparison with coastal AIS has been published (Helleren et al., 2012b). The best fit was found for moving ships in open ocean areas, away from land-based interference; see Fig. 10 for a comparison. The fit is best for moving ships since the AIS system then requires the ships to transmit a large number of AIS messages during a typical satellite pass. Stationary ships transmit messages less often, decreasing the probability of reception by the space-based AIS system. Typically ships are not stationary when in the open oceans, and closer to land the alternative data sources provide good coverage. Since ships that are

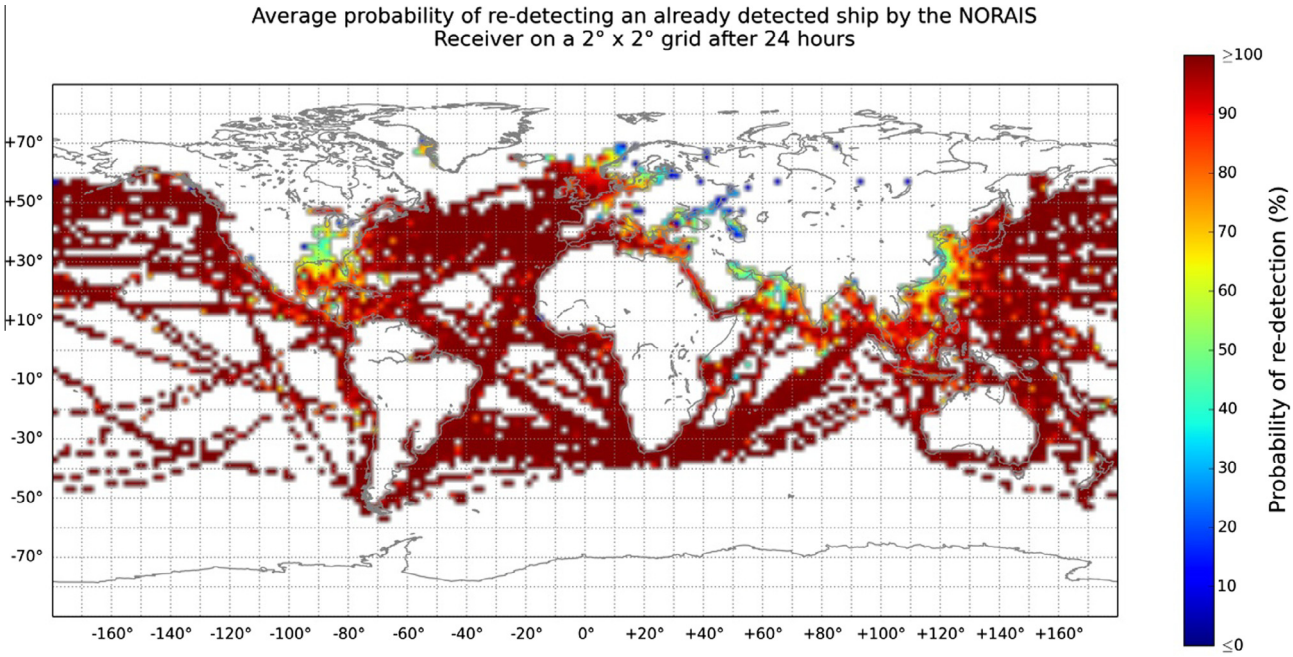

Fig. 9. Statistically accumulated average probability of re-detecting an already detected ship using the AIS3 and AIS4 channels by the NORAIS Receiver within 24 h.

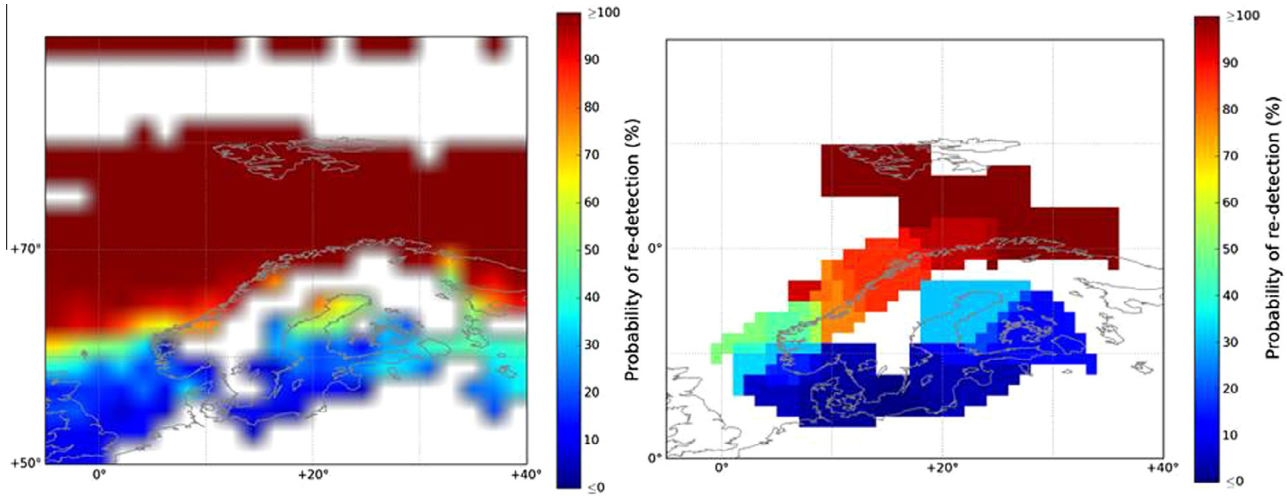

Fig. 10. Probability of re-detecting an already detected ship by AISSat-1 within 12 h (left) and AISSat-1 detection performance from comparison with coastal AIS data (Helleren et al., 2012b) within 7 passes, ca. 11 h 30 min (right), using the AIS1 and AIS2 channels.

never detected do not contribute to the re-detection probability, the results in the difficult high traffic zones close to and including the North Sea, English Channel, Baltic Sea, Mediterranean Sea, Black Sea, East and South China Sea, Sea of Japan and to an extent the Gulf of Mexico is exaggerated.

While the AISSat and NORAIS receivers have had algorithm upgrades since their original development in 2008, even more advanced algorithms have been developed since then (Burzigotti et al., 2012; Hassanin et al., 2015). The improved algorithms should improve the tracking capability of the next generation space-based AIS system significantly beyond the capability presented in this paper. A NORAIS-2 Receiver hardware upgrade replaced the NORAIS Receiver in February 2015 to demonstrate next generation algorithms. The algorithms operate across all four AIS channels simultaneously, which on its own will improve the tracking capability of the system. In addition, the NORAIS-2 Receiver also has the capacity to sample the raw signal for an entire orbit for detailed processing on ground to investigate the nature of the sources of interference and benchmark alternative algorithms with recordings of a real in-orbit signal environment. The NORAIS-2 Receiver project is, like the NORAIS Receiver project, led by FFI with support from ESA's General Support Technical Programme during the development phase, and ESA's

PRODEX programme (PROgramme de Développement d'Expériences scientifiques) during the operational phase. The AIS receiver itself is once again also from Kongsberg Seatex and is based on their heritage work that eventually led to their latest generation receiver design developed in ESA's ARTES 21 SAT-AIS programme (ESA, 2015).

Other methods to improve the space-based AIS system performance compared with the results presented in this paper are the use of multiple antennas in order to increase the probability of detecting messages that have experienced significant polarisation rotation (Helleren et al., 2008; Zhou et al., 2012; Picard et al., 2012; Maggio et al., 2014). The rotation reduces the signal strength below the required signal-to-noise ratio for an antenna of the same polarisation as the transmission antenna. Two, or three, cross polarised monopole antennas will be able to account for more polarisation rotation of the messages, while at the same time individually suppressing overlapping messages of different polarisation rotation.

Section 3.2 demonstrated the effect of adding a second satellite to a space-based AIS system, and Section 4 demonstrated the effect of the new space AIS channel, AIS3 and AIS4. The tracking capability after 24 h showed a greater improvement in the high traffic zones when operating on the space AIS channels compared with adding a second satellite to the space-based AIS system.

Determining which of the four methods (improving algorithms, multiple/better antennas, adding satellites or focussing on the space AIS channels) that will yield the greatest system performance improvement is not straightforward and depends on the end-user requirements. When more ships start to use the space AIS channels, the tracking capability of a space-based AIS system is most improved by decoding on these new channels. Adding a second satellite (or more) can have a larger positive impact on the time update interval and overall system redundancy than any of the other methods for improvement mentioned. Better algorithms and/or multiple/better antennae will result in more messages per ship, which can be used in value added services such as independent verification of the reported position from frequency shift estimation and data fusion (Skauen et al., 2013). Furthermore, in Section 2.4 it was argued that some ships always have transmitted signal strengths too low to be received by a space-based AIS system and inspecting and overhauling the ship AIS equipment itself will be the best way to improve the ship detection probability by a space-based AIS system.

6. Summary

A method for assessing the tracking capability of a space-based AIS system was presented. The method was applied to both the single satellite AISSat-1 system and the two-satellite AISSat-1 and AISSat-2 constellation. The results show the effectiveness of a space-based AIS system in providing a global maritime picture, though the high ship density areas are challenging. The expected improvement from operation on the space AIS channels was also presented based on NORAIS Receiver data. Operating on the space AIS channels, the re-detection probability in the high ship density areas is markedly improved.

The derived re-detection probability was justified to represent an upper bound on the space-based AIS system performance and a best fit for moving ships in the high seas. The most important caveat of the method was that ships that are never detected, and should contribute negatively to the re-detection probability, are naturally not included. The high traffic zones close to and including the North Sea, English Channel, Baltic Sea, Mediterranean Sea, Black Sea, East and South China Sea, Sea of Japan and to an extent the Gulf of Mexico are most impacted and the reported re-detection probability is exaggerated as a result. In addition there were some edge effects both with respect to time and area that also affect the results.

Acknowledgements

The operations of the NORAIS Receiver and the analysis of NORAIS Receiver data presented in this paper is supported by the European Space Agency – Norway through their PRODEX (PROgramme de Développement d'Expériences scientifiques) programme (PRODEX Experiment Arrangement 40001000590 "COLAIS")

The NORAIS algorithm development by Kongsberg Seatex was supported by the European Space Agency through the General Support Technology Programme (GSTP) (ESTEC/Contract No. 4000103368).

References

Burzigotti, P., Ginesi, A., Colavolpe, G., 2012. Advanced receiver design for satellite-based automatic identification system signal detection. Int. J. Satell. Commun. Networking 30, 52–63. http://dx.doi.org/10.1002/sat.107.

Carson-Jackson, J., 2012. Satellite AIS – developing technology or existing capability? J. Navig. 65 (2), 303–321. http://dx.doi.org/10.1017/S037346331100066X.

Chen, Y., 2014. Satellite-based AIS and its comparison with LRIT. Int. J. Mar. Navig. Saf. Sea Transp. 8 (2). http://dx.doi.org/10.12716/1001.08.02.02.

Commission implementing regulation (EU), 2011. No 404/2011 of 8 April 2011 laying down detailed rules for the implementation of Council Regulation (EC) No 124/2009 establishing a Community control system for ensuring compliance with the rules of the Common Fisheries Policy.

Dembovskis, A., 2012. Testbed for performance evaluation of SAT-AIS receivers. In: Proceedings of the Advanced Satellite Multimedia Systems Conference (ASMS) and the 12th Signal Processing for Space Communications Workshop (SPSC), pp. 253–257. doi: 10.1109/ASMS-SPSC.2012.6333085.

Eriksen, T., Høye, G., Narheim, B., Meland, B.J., 2006. Maritime traffic monitoring using a space-based AIS receiver. Acta Astronaut. 58 (10), 537–549. http://dx.doi.org/10.1016/j.actaastro.2005.12.016.

Eriksen, T., Skauen, A., Narheim. B., Helleren, Ø., Olsen, Ø., Olsen, R., 2010. Tracking ship traffic with space-based AIS: experience gained in first months of operations. In: Proceedings of the Waterside Security Conference, Marina di Carrara, Italy. doi: 10.1109/WSSC.2010.5730241.

European Space Agency (ESA), 2009. Atlantis leaves Columbus with a radio eye on Earth's sea traffic. Available from: <http://www.esa.int/Our_Activities/Operations/i_Atlantis_i_leaves_Columbus_with_a_radio_eye_on_Earth_s_sea_traffic> [Accessed 22 September 2015].

European Space Agency (ESA), 2015. Novel SAT-AIS Receiver Phase B2/C/D. Available from: <https://artes.esa.int/projects/novel-sat-ais-receiver-phase-b2cd> [Accessed 9 October 2015].

Hassani, A., Lazaro, F., Plass, S., 2015. An advanced AIS receiver using a priori information. In: Proceedings of the OCEANS 2015 Conference, Genova, Italy. doi: 10.1109/OCEANS-Genova.2015.7271475.

Helleren, Ø., Olsen, Ø., Berntsen, P.C., Strauch, K., Alagha, N., 2008. Technology reference and proof-of-concept for a space-based automatic identification system for maritime security. In: Proceedings of the 4S Symposium, Rhodes, Greece.

Helleren, Ø., Olsen, Ø., Narheim, B.T., Skauen, A.N., Olsen, R.B., 2012a. AISSat-1 – 2 years of service. In: Proceedings of the 4S Symposium, Portorož, Slovenia.

Helleren, Ø., Eriksen, T., Olsen, R.B., Narheim, B.T., Skauen, A.N., Olsen, Ø., Svenes, K.R., 2012b. Extending maritime situational awareness with satellite-based AIS. In: Proceedings of the North Atlantic Treaty Organisation (NATO) Research and Technology Organisation SCI-247 Symposium on Port and Regional Maritime Security, Lerici, Italy. (NATO UNCLASSIFIED).

International Telecommunication Union (ITU), 2009. Recommendation ITU-R M.2169 – improved satellite detection of AIS.

International Telecommunication Union (ITU), 2014. Recommendation ITU-R M.1372-5 – technical characteristics for an automatic identification system using time division multiple accessing the VHF maritime mobile frequency band.

Maggio, F., Rossi, T., Cianca, E., Ruggieri, M., 2014. Digital beamforming techniques applied to satellite-based AIS receiver. IEEE Aerosp. Electron. Syst. Mag. 29 (6), 4–12. http://dx.doi.org/10.1109/MAES.2014.130168.

Nakamura, Y., Nishijo, K., Murakami, N., Kawashima, K., Horikawa, Y., Yamamoto, K., Ohtani, T., Takhashi, Y., Inoue, K., 2013. Small demonstration satellite-4 (SDS-4): development, flight results, and lessons learned in JAXA's microsatellite project. In: Proceedings of the AIAA/USU Conference on Small Satellites, The Year in Review, SSC13-X-1. <http://digitalcommons.usu.edu/smallsat/2013/all2013/113/>.

Narheim, B.T., Helleren, Ø., Olsen, Ø., Olsen, R., Rosshaug, H., Beattie, A.M., Kekez, D.D., Zee, R.E., 2011. AISSat-1 early results. In: Proceedings of the AIAA/USU Conference on Small Satellites, Reflections on the Past, SSC11-III-6. <http://digitalcommons.usu.edu/smallsat/2011/all2011/26/>.

Picard, M., Oularbi, M.R., Flandin, G., Houcke, S., 2012. An adaptive multi-user multi-antenna receiver for satellite-based AIS detection. In: Proceedings of the Advanced Satellite Multimedia Systems Conference (ASMS) and the 12th Signal Processing for Space Communications Workshop (SPSC), pp. 273–280. doi: 10.1109/ASMS-SPSC.2012.6333088.

Posada, M., Greidanus, H., Alvarez, M., Vespe, M., Cokacar, T., Falchetti, S., 2011. Maritime awareness for counter-piracy in the gulf of aden. In: Proceedings of 2011 International Geoscience & Remote Sensing Symposium, pp. 249–252. doi: 10.1109/IGARSS.2011.6048939.

Re, E., Boissinot, V., Ginesi, A., Tobehn, C., 2012. A simple high precision method for extrapolating SAT-AIS system performance. In: Proceedings of the Advanced Satellite Multimedia Systems Conference (ASMS) and the 12th Signal Processing for Space Communications Workshop (SPSC), pp. 266–272. doi: 10.1109/ASMS-SPSC.2012.6333087.

Skauen A.N., Helleren, Ø., Olsen, Ø., Olsen, R., 2013. Operator and user perspective of fractionated AIS satellite systems. In: Proceedings of the AIAA/USU Conference on Small Satellites, Around the Corner, SSC13-XI-5. <http://digitalcommons.usu.edu/smallsat/2013/all2013/123/>.

Skauen A.N., Olsen, Ø., 2015. Signal environment mapping of the Automatic Identification System frequencies from space. *Advances in Space Research*, unpublished manuscript.

Zhou, M., van der Veen, A.-J., van Leuken, R., 2012. Multi-user LEO-satellite receiver for robust space detection of AIS messages. In: Proceedings of the 2012 IEEE Conference on Acoustics, Speech and Signal Processing (ICASSP), pp. 2529–2532. doi: 10.1109/ICASSP.2012.6288431.